

Hyperentanglement of two photons in three degrees of freedom

Giuseppe Vallone,^{1,*} Raino Ceccarelli,^{1,*} Francesco De Martini,^{1,2} and Paolo Mataloni^{1,*}

¹ *Dipartimento di Fisica della Sapienza Università di Roma, Roma, 00185 Italy and
Consorzio Nazionale Interuniversitario per le Scienze Fisiche della Materia, Roma, 00185 Italy*

² *Accademia Nazionale dei Lincei, via della Lungara 10, Roma 00165, Italy**

(Dated: November 6, 2018)

A 6-qubit hyperentangled state has been realized by entangling two photons in three degrees of freedom. These correspond to the polarization, the longitudinal momentum and the indistinguishable emission produced by a 2-crystal system operating with Type I phase matching in the spontaneous parametric down conversion regime. The state has been characterized by a chained interferometric apparatus and its complete entangled nature has been tested by a novel witness criterium specifically introduced for hyperentangled states. The experiment represents the first realization of a genuine hyperentangled state with the maximum entanglement between the two particles allowed in the given Hilbert space.

PACS numbers: 03.67.Bg, 42.50.Dv, 42.65.Lm

Keywords: hyperentanglement, spontaneous parametric down conversion, multiqubit photon states

Hyperentangled (HE) 2-photon states, i.e. quantum states of two photons simultaneously entangled in N independent degrees of freedom (DOF's) [1, 2], are nowadays recognized as a basic resource for many quantum information (QI) processes. At variance with n -photon entanglement, hyperentanglement is much less affected by decoherence and the detection efficiency of the state scales by η^n , with η the quantum efficiency of detectors, is not reduced by growing the size of the state.

Important quantum communication protocols have been demonstrated by using two photon HE states, such as enhancing the channel capacity in superdense coding [3] and the complete and deterministic discrimination of the four orthogonal polarization Bell states [4, 5]. Hyperentanglement is also a viable resource in view of enhancing the power of computation of a scalable one-way quantum computer [6]. Indeed, by applying suitable transformations on the HE states, efficient 4-qubit 2-photon cluster states were created [7] and used in the realization of basic quantum computation algorithms [8, 9]. Finally, working in a large dimension Hilbert space with N entangled DOF's of the photons allows to perform advanced tests of quantum nonlocality able to largely enhance the violation of local realism [10, 11, 12].

HE states of increasing size are of paramount importance for the realization of even more challenging QI objectives. Recently, optical schemes involving two or more photons were proposed to expand the available Hilbert space to incredibly large dimensions. In particular three DOF's of the photons, namely polarization, spatial mode, and time-energy, were used to build a multidimension entangled state of two photons encoded in four qubits and two qutrits [13]. More recently, Greenberger-Horne-Zeilinger (GHZ) states of up to 10-qubits were engineered by exploiting polarization and momentum of five pho-

tons [14]. It is worth noting that in both experiments the addition of one DOF, i.e. time-energy and linear momentum, respectively, derives from a local manipulation¹ of polarization entanglement that enhances the number of DOF's without increasing the entanglement between the particles. Indeed, in both experiments the entanglement of the additional DOF was not independent from the polarization entanglement².

We can fully take advantage of an enlarged Hilbert space by independently entangling the two photons in N DOF's in order to create a “genuine” HE state, given by the product of N Bell states,

$$|\Psi_N\rangle = |\text{Bell}_1\rangle \otimes |\text{Bell}_2\rangle \otimes \cdots \otimes |\text{Bell}_N\rangle \quad (1)$$

one for each DOF [16].

Let's consider the *entropy of entanglement* of the state $|\Psi_N\rangle$,

$$E(|\Psi_N\rangle) = S[\text{tr}_A(|\Psi_N\rangle\langle\Psi_N|)] = S[\text{tr}_B(|\Psi_N\rangle\langle\Psi_N|)], \quad (2)$$

where S is the standard Von-Neumann entropy, defined as $S(\rho) = -\text{tr}(\rho \log_2 \rho)$. It's easy to demonstrate that $E(|\Psi\rangle) = N$, independently of any local operation. Hence the state $|\Psi\rangle$ allows to maximize the degree of entanglement of two particles for a given Hilbert space. On the other hand, by adding other DOF's to the state by local operations, the entropy of entanglement doesn't change, as said.

¹ We define local manipulation any transformation that acts separately on each particle.

² In the experiment of Ref. [13] two Franson-type polarization interferometers, one for each photon and each one realized by a quartz birefringent element, were used to analyze time-energy entanglement. The entanglement due to the polarization and time-energy DOF's could be made really “independent” and thus the total entanglement of the state could grow by using standard Franson-type unbalanced interferometers [15].

*URL: <http://quantumoptics.phys.uniroma1.it/>

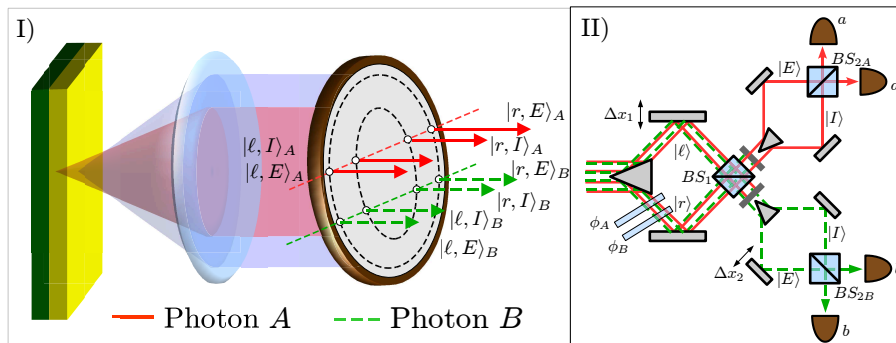


FIG. 1: Experimental setup. I) The 2-crystal system generates photon pairs with equal probability over the internal (I) and external (E) cone. Polarization entanglement arises from double passage of the pump beam through the crystals and the combined action of a spherical mirror and a $\lambda/4$ wave-plate (not shown in the figure). The annular sections of each emission cone, with diameters $d_I = 12\text{mm}$ and $d_E = 16\text{mm}$ are intercepted by a single 8-hole screen. II) Measurement setup: the first interferometer (ending with BS_1) measures momentum entanglement in the basis $\frac{1}{\sqrt{2}}(|\ell\rangle + e^{i\phi_{A,B}}|r\rangle)$, at the same time for Alice (red line) and Bob (dotted green line) photon. Phase ϕ_A (ϕ_B) is set by tilting a thin glass plate intercepting the Alice (Bob) mode. The subsequent interferometers, corresponding to BS_{2A} and BS_{2B} , perform the measurement separately for the Alice and Bob photon in the basis $\frac{1}{\sqrt{2}}(|I\rangle \pm |E\rangle)$. The interference filters allowing photon detection within a bandwidth $\Delta\lambda = 6\text{nm}$ and the four apparatus for polarization analysis aligned before each detector are not shown in the figure.

In this Letter we present the experimental realization and characterization of a 6-qubit HE state based on the simultaneous triple entanglement of two photons. By our scheme, besides polarization (π) entanglement, two photons experience a further double entanglement in the longitudinal momentum DOF. In the experiment this was done by selecting four pairs of correlated \mathbf{k} -modes within the spatial emission of a two-crystal system operating in the spontaneous parametric down conversion (SPDC) regime. This configuration realizes a genuine 2-photon HE state with $E = 3$ and thus entangled in $N = 3$ independent DOF's, labelled as π , \mathbf{k} and \mathbf{c} .

In the experiment we adopted a 2-crystal geometry to generate the 6-qubit HE state. Precisely, two 0.5 mm thick Type I β -barium-borate (BBO) crystal slabs, cut at different phase matching angles, (see Figure 1-I), aligned one behind the other, were operating under double excitation (back and forth) of a vertically (V) polarized continuous wave (CW) laser at wavelength λ_p .

The polarization entangled Bell state $|\Phi^-\rangle = \frac{1}{\sqrt{2}}(|H\rangle_A|H\rangle_B - |V\rangle_A|V\rangle_B)$ was created by spatial superposing the two perpendicularly polarized emission cones of each Type I crystal, in agreement with a method already described by us in previous papers [2].

Photon pairs were created with equal probability at degenerate wavelength $\lambda = 2\lambda_p$ by either one of BBO crystals along two correlated directions belonging to the lateral surfaces of two SPDC cones, with full aperture angles $\theta_I = 4.6^\circ$ and $\theta_E = 6.1^\circ$, respectively. We refer to them as the “internal” (I) and the “external” (E) cone, corresponding to the first and the second crystal, respectively. The dichotomy existing between the I and E cone “photon choice” is thus identified as a third independent DOF in the state. Coherence and hence indistinguishability between the two crystal emissions is guaranteed

by the the fact that the pump coherence length exceeds by more than one order of magnitude the total crystal length.

The two conical emissions were then transformed into two cylindrical ones by a positive lens with focal length $f = 15\text{cm}$, located at a distance f from the intermediate point of the 2-crystal device. Double longitudinal momentum entanglement was created by selecting four pairs of correlated modes with a 8-hole screen. Precisely, the following correlated mode pairs, $|I, \ell\rangle_A - |I, r\rangle_B$, $|I, r\rangle_A - |I, \ell\rangle_B$ were selected for the first crystal and $|E, \ell\rangle_A - |E, r\rangle_B$, $|E, r\rangle_A - |E, \ell\rangle_B$ for the second crystal emission. It is worth to remember that only two photons, namely A (Alice) and B (Bob), are generated with equal probability by either one of the crystals. We label the corresponding mode emission as ℓ (r) by referring to the left (right) side of each cone and as I (E) by considering the internal (external) cone (see Figure 1-I).

The produced state is given by the product of one polarization entangled state and two longitudinal momentum entangled states (or, equivalently, two ququart entangled state) and is expressed as a 6-qubit HE state:

$$\frac{1}{\sqrt{2}} (|H\rangle_A|H\rangle_B + e^{i\varphi\pi}|V\rangle_A|V\rangle_B) \otimes \frac{1}{\sqrt{2}} (|\ell\rangle_A|r\rangle_B + e^{i\varphi\mathbf{k}}|r\rangle_A|\ell\rangle_B) \otimes \frac{1}{\sqrt{2}} (|I\rangle_A|I\rangle_B + e^{i\varphi\mathbf{c}}|E\rangle_A|E\rangle_B) \quad (3)$$

It's easy to verify that the entropy of entanglement of this state equals exactly the number of DOF's $N = 3$. It corresponds to the maximum allowed entanglement for a $2^3 \times 2^3$ Hilbert space, as said.

The measurement setup used to test the triple entanglement was given by the chained interferometric apparatus sketched in Figure 1-II). It is divided in two parts: the first one performs the measurement of the momentum

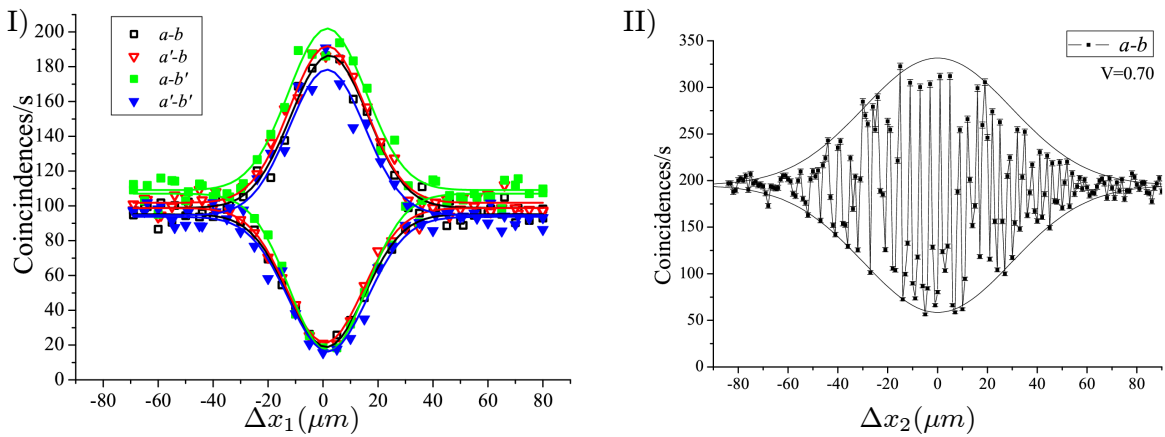


FIG. 2: I) Coincidence rates $a-b$, $a'-b$, $a-b'$, $a'-b'$ vs Δx_1 for the state (3) showing the typical dip- ($\varphi_{\mathbf{k}} = 0$) peak ($\varphi_{\mathbf{k}} = \pi$) feature with average visibility $V = 0.815 \pm 0.022$ (dip) and $V = 0.877 \pm 0.031$ (peak). The corresponding experimental fits are also shown. FWHM $\simeq 30\text{nm}$ of the interference patterns is in agreement with the expected value for a filter bandwidth of 6 nm. II) Coincidence rate $a-b$ vs Δx_2 for the state (3) with $\varphi_{\mathbf{k}} = \pi$ with visibility $V \simeq 0.70$ and FWHM $\simeq 60$ nm. In both cases the time average of each experimental point is 3s.

entanglement existing within each emission cone. Here the ℓ modes are spatially and temporally matched with the r modes both for the up- (A photon) and down- (B photon) side of a common 50:50 beam splitter (BS_1), for both the I and E emission cone. In the second part of the apparatus, measuring momentum entanglement between the two crystal emissions, the left (right) BS_1 output modes belonging to the Alice (Bob) photon are then injected in another interferometer where the I and E modes are matched onto the BS_{2A} (BS_{2B}) beam splitter.

Two trombone mirror assemblies mounted on motorized translation stages allow fine adjustment of path delays Δx_1 and Δx_2 between the different mode sets in the first and second part of the interferometric apparatus. Phase setting of \mathbf{k} momentum entanglement is achieved by careful tilting of thin glass plates ϕ_A and ϕ_B , placed respectively on the Alice and Bob right modes (cfr. Fig. 1-II).

Four single photon detectors, mod. Perkin Elmer SPCM-AQR14, detect the radiation belonging to the Alice output modes of BS_{2A} , namely a and a' in Figure 1-II), and to the Bob output modes of BS_{2B} (b and b' in Figure 1-II)). Polarization entanglement is measured by using four standard polarization analyzers, one for each detector.

The experimental results given in Figure 2-I) show the characteristic interference patterns obtained by measuring the coincidences $a-b$, $a-b'$, $a'-b$ and $a'-b'$ as a function of Δx_1 . Momentum entanglement is demonstrated by the typical dip-peak transition obtained by adjusting the state phase. In the same way, similar interference traces were obtained for the four sets of coincidences by varying the delay Δx_2 in the second interferometer. We show in Figure 2-II) the one corresponding to the measurement of $a-b$ coincidences.

We can observe the different effect on phase stability

appearing in the figures: in the first interferometer ($|\ell\rangle$ - $|r\rangle$ measurement) the phase $\varphi_{\mathbf{k}}$ is self-stabilized since any mirror instability corresponds to a global phase variation of the state. Moreover, since any change of Δx_1 determines the simultaneous variation of all the $|r\rangle$ mode optical delays, even in this case the phase remains constant. This features is evident in Fig. 2-I), where we show the different coincidence patterns for $\varphi_{\mathbf{k}} = 0$ and $\varphi_{\mathbf{k}} = \pi$.

In the second interferometer ($|I\rangle$ - $|E\rangle$ measurement) the phase $\varphi_{\mathbf{c}}$ is not self-stabilized and a compact interferometer is needed to achieve high phase stability. Moreover, the variation of Δx_2 changes only the $|E\rangle$ path delay of the B photon. This corresponds in Fig. 2-II) to a random $\varphi_{\mathbf{c}}$ phase variation. For the same reason the full width half maximum (FWHM) duration of the interference pattern of Fig. 2-II) doubles the one of Figure 2-I).

We detected the entanglement present in the generated HE state by using a novel criterium recently proposed for hyperentanglement [16]. It is based on the evaluation of some witnesses specifically introduced for graph states.

Let's describe how the hyperentanglement test was carried out. For each DOF spanning a two dimensional Hilbert space, we associate the states $|H\rangle$, $|\ell\rangle$ and $|I\rangle$ to the basis vector $|0\rangle$, while $|V\rangle$, $|r\rangle$ and $|E\rangle$ are associated to $|1\rangle$. By setting all the phases φ_{μ} (with $\mu = \pi, \mathbf{k}, \mathbf{c}$) to zero we obtain the following HE state:

$$|\Psi_3\rangle = |\phi^+\rangle_{\pi} \otimes |\psi^+\rangle_{\mathbf{k}} \otimes |\phi^+\rangle_{\mathbf{c}} \quad (4)$$

with the standard Bell states $|\phi^+\rangle = \frac{1}{\sqrt{2}}(|0\rangle_A|0\rangle_B + |0\rangle_A|1\rangle_B)$ and $|\psi^+\rangle = \frac{1}{\sqrt{2}}(|0\rangle_A|1\rangle_B + |1\rangle_A|0\rangle_B)$. We also define Z_i , z_i and z'_i ($i = A, B$) the σ_z Pauli matrices for the π , \mathbf{k} and \mathbf{c} DOF respectively. Similarly, X_i , x_i and x'_i represent the corresponding σ_x matrices.

We first verified the presence of entanglement between the two photons for each separate DOF. This was done

S_1	S_2	S_3	S_4
0.733 ± 0.006	0.897 ± 0.005	0.810 ± 0.005	0.989 ± 0.002
S_5	S_6	$S_1 S_3$	$S_1 S_5$
0.420 ± 0.008	0.990 ± 0.002	0.681 ± 0.007	0.443 ± 0.008
$S_3 S_5$	$S_1 S_3 S_5$	$S_2 S_4 S_6$	$S_2 S_4$
0.398 ± 0.008	0.445 ± 0.008	0.891 ± 0.005	0.893 ± 0.005
$S_2 S_6$	$S_4 S_6$		
0.895 ± 0.005	0.988 ± 0.002		

TABLE I: Experimental values of the operators needed to measure W_π , $W_{\mathbf{k}}$, $W_{\mathbf{c}}$, W_2 , and W_3 .

by tracing the other DOF's and evaluating separately an entanglement witness for π , \mathbf{k} and \mathbf{c} entanglement. Let's define the following witnesses:

$$W_\pi = (\mathbb{1}_\pi - 2X_A X_B - 2Z_A Z_B) \otimes \mathbb{1}_{\mathbf{k}} \otimes \mathbb{1}_{\mathbf{c}} \quad (5a)$$

$$W_{\mathbf{k}} = \mathbb{1}_\pi \otimes (\mathbb{1}_{\mathbf{k}} - 2x_A x_B - 2z_A z_B) \otimes \mathbb{1}_{\mathbf{c}} \quad (5b)$$

$$W_{\mathbf{c}} = \mathbb{1}_\pi \otimes \mathbb{1}_{\mathbf{k}} \otimes (\mathbb{1}_{\mathbf{c}} - 2x'_A x'_B - 2z'_A z'_B) \quad (5c)$$

The negative experimental values, $W_\pi = -0.6298 \pm 0.0080$, $W_{\mathbf{k}} = -0.7987 \pm 0.0055$ and $W_{\mathbf{c}} = -0.4101 \pm 0.0082$ demonstrate the entanglement in each DOF.

As explained in [16], these measurement are not sufficient to ensure that the prepared state is a genuine HE state. Indeed there are states with negative values of W_π , $W_{\mathbf{k}}$ and $W_{\mathbf{c}}$ that can be prepared by a classical mixture of several simple entangled (i.e. entangled in only one DOF) states. We then need to measure a witness able to detect the global entanglement of the HE state. It has been demonstrated [16] that the following operators can be used in our case:

$$W_2 = 3 - 2 \left(\prod_{k=1}^3 \frac{S_{2k} + 1}{2} + \prod_{k=1}^3 \frac{S_{2k-1} + 1}{2} \right) \quad (6)$$

$$W_3 = 2 - 3 \prod_{k=1}^3 \left(\frac{1 + S_{2k-1} + S_{2k}}{3} \right) \quad (7)$$

where $S_1 = X_A X_B$, $S_2 = Z_A Z_B$, $S_3 = x_A x_B$, $S_4 = -z_A z_B$, $S_5 = x'_A x'_B$ and $S_6 = z'_A z'_B$ are the *stabilizers* of the hyperentangled state (4). The expectation value of both the witnesses is equal to -1 for a pure triple HE state. The difference between W_2 and W_3 resides on the respective numbers of measurement settings and on their resistance to white noise. In particular W_3 is more demanding than W_2 since it requires a larger number of settings but, at the same time, it is more resistant to noise. The measured values of the witnesses, $W_2 = -0.1182 \pm 0.0055$ and $W_3 = -0.0890 \pm 0.0037$, obtained by the experimental values of the operators shown in Table I, demonstrate that the whole produced state is entangled and thus represents a genuine HE state.

In conclusion, we experimentally demonstrated the simultaneous entanglement of two photons by using three independent DOF's, corresponding to the polarization and two different longitudinal momentum deriving by the indistinguishable emission of two nonlinear crystals. The existence of entanglement of the state was demonstrated by using an entanglement witness method specifically introduced for HE state. Our results represent the first realization of a 2-photon 6-qubit HE state with the maximum achievable entanglement for a state involving three DOF's. Since the number of \mathbf{k} -modes involved in Type I emission processes is virtually infinite, HE states with even larger size are expected by using longitudinal momentum entanglement but at the price of a large number of \mathbf{k} -modes in which the photons can be detected. Other DOF's can be exploited in the future, such as energy-time [15, 17] or orbital angular momentum [13], to create larger multidimension entangled states of two photons suitable for novel advanced QI tasks.

We thank A. Cabello for useful discussions.

-
- [1] P. G. Kwiat, J. Mod. Opt. **44**, 2173 (1997).
[2] M. Barbieri, C. Cinelli, P. Mataloni, and F. De Martini, Phys. Rev. A **72**, 052110 (2005).
[3] J. T. Barreiro, T.-C. Wei, and P. G. Kwiat, Nature (London) **4**, 282 (2008).
[4] M. Barbieri, G. Vallone, P. Mataloni, and F. De Martini, Phys. Rev. A **75**, 042317 (2007).
[5] C. Schuck, G. Huber, C. Kurtsiefer, and H. Weinfurter, Phys. Rev. Lett. **96**, 190501 (2006).
[6] H. J. Briegel and R. Raussendorf, Phys. Rev. Lett. **86**, 910 (2001). R. Raussendorf and H. J. Briegel, *ibid.* **86**, 5188 (2001).
[7] G. Vallone, E. Pomarico, P. Mataloni, F. De Martini, and V. Berardi, Phys. Rev. Lett. **98**, 180502 (2007).
[8] K. Chen *et al.*, Phys. Rev. Lett. **99**, 120503 (2007).
[9] G. Vallone, E. Pomarico, F. De Martini, and P. Mataloni, Phys. Rev. Lett. **100**, 160502 (2008).
[10] M. Barbieri, F. De Martini, P. Mataloni, G. Vallone, and A. Cabello, Phys. Rev. Lett. **97**, 140407 (2006).
[11] D. Collins, N. Gisin, N. Linden, S. Massar, and S. Popescu, Phys. Rev. Lett. **88**, 040404 (2002).
[12] A. Cabello, Phys. Rev. Lett. **97**, 140406 (2006).
[13] J. T. Barreiro, N. K. Langford, N. A. Peters, and P. G. Kwiat, Phys. Rev. Lett. **95**, 260501 (2005). E. Nagali *et al.*, (2008), [arXiv:0810.2417]
[14] W.-B. Gao *et al.*, (2008), [arXiv:0809.4277].
[15] J. D. Franson, Phys. Rev. Lett. **62**, 2205 (1989).
[16] G. Vallone, R. Ceccarelli, F. De Martini, and P. Mataloni, (2008), [arXiv:0809.2155].
[17] A. Rossi, G. Vallone, F. De Martini, and P. Mataloni, Phys. Rev. A **78**, 012345 (2008).